

Load Frequency Controller Design for Microgrid using Internal Model Control Approach

A.Jeya Veronica *, Dr. N.Senthil Kumar **‡,

* Research Scholar, School of Electrical Engineering, VIT University, Chennai Campus, Vandalur-Kelambakkam Road,
Chennai-600127

** Associate Professor, School of Electrical Engineering, VIT University, Chennai Campus, Vandalur-Kelambakkam Road,
Chennai-600127

(jeya.veronicaa2014phd1162@vit.ac.in, senthilkumar.nataraj@vit.ac.in)

‡ Corresponding Author; Dr. N.Senthil Kumar, VIT University, Chennai Campus, Vandalur-Kelambakkam Road, Chennai-
600127, Tamilnadu, India, Tel:9444242263,

Received: 23.11.2016 Accepted: 06.02.2017

Abstract- The impact of renewable energy sources is no longer negligible in microgrid when high penetration levels are required. This paper explores load frequency control issues in a microgrid comprising of wind turbine generators(WTG), diesel generators(DG), fuel cells(FC) fed by aqua electrolyzers(AE) and battery energy storage systems(BESS). Due to the interconnection of these intermittent energy sources the microgrid frequency deviates. To enhance better frequency regulation in the microgrid, proportional integral(PI) controllers are used for controlling the real power generation of these micro sources. It is observed that the system frequency regulation improves considerably by utilizing PI Controllers tuned using internal model control(IMC) approach. This paper explores the design procedure of IMC tuned PI controllers and fractional order PI(FOPI) controllers for micro grid systems. The robustness of the IMC based PI Controllers have been verified by changing the parameters of the microgrid sources.

Keywords Frequency control, microgrid, Fractional Order PI controller, Internal Model Control design.

1. Introduction

Power generation over the past decade has moved from centralized fossil fuel fired thermal power plants to power generating sources consisting of renewable energy sources located closer to the customers. This arrangement reduces the transmission losses of the system, provides better controllability satisfying their power demands. However, due to the intermittent nature of the renewable sources used with these hybrid microgrids the system frequency deviations are appreciably high. To settle down the system frequency closer to nominal values, synthesizing of better control techniques are required with these energy sources to control the power generation.

Because of the depleting nature of fossil fuels and energy crisis existing in conventional power systems, small power generating units consisting of renewable resources are formed. Such power generating sources located closer to load centers are termed microgrids. The intermittent nature of the

renewable sources used in microgrids results in frequency fluctuations. A microgrid could be formed by combining renewable sources like wind, solar, FC and other sources like BESS and DG.

With the appropriate control of generation of power from these sources, generation ,load balance is achieved which results in reduced frequency deviations [1,2]. As the wind power is intermittent, frequency deviations could be reduced by using FC for long time and flywheel for short time energy storage [3]. BESS combined with other renewable energy sources are used to reduce the system frequency deviations [4]. The size of BESS is optimized to act as a primary reserve in which the frequency deviations in a microgrid are minimized [5]. Wind energy is inconsistent in nature and interconnection of it in the microgrid causes frequency deviations. A coordinated control strategy has been proposed such that the WTG and BESS are coordinated to control the frequency deviations [6]. A combination of small hydro power plant connected to synchronous generator, WTG,

BESS and an electronically controlled smart load is used for frequency control [7]. Frequency deviation occurs due to the changes in the renewable energies and load. A robust control method has been proposed for the microgrid in which the BESS is attached [8].

The BESS plays a major role in load frequency control. When the system frequency is less than the nominal value, the BESS discharges and charges when the system frequency is greater than the nominal value. The model predictive control(MPC) method has been used for the optimal operation of BESS for frequency control [9]. In islanded microgrid, to deliver consistent supply, frequency control is essential. The voltage source converter associated with the BESS is controlled using affine projection-like algorithm for frequency control [10]. The inequality between the power supply and the demand is responsible for instability of frequency in islanded microgrids. To maintain the frequency within the permissible range, an adaptive load shedding scheme for frequency stability has been proposed[11]. As the load and generating power of the renewable energy sources differ, the microgrid frequency fluctuates. A robust control technique termed H_∞ and μ -Synthesis methods have been implemented for effective frequency control loop [12].

PID controllers ensure that the performance of the overall plant results in reduced settling time and peak overshoots following a disturbance. A better control performance can be obtained if the controller parameters are tuned optimally. A self tuning algorithm for PI controllers has been proposed which is centered on the emotional learning process by the human brain [13]. With the growing number of microgrids, maintaining the balance between generation and demand has become an important issue. The PI controllers tuned using classical tuning methods are not robust and appropriate for all the operating conditions. A new on-line intelligent method to tune PI controllers using fuzzy logic and particle swarm optimization(PSO) technique has better control over the frequency deviations [14]. To minimize the battery usage and control the microgrid frequency effectively robust PI controllers are used and tuned using genetic algorithms(GA) [15]. The feasibility of FC and AE control to ensure real power balance and improve frequency regulation is examined [16]. Ziegler Nichols(ZN) method is suggested to tune PI controllers for reducing the frequency deviations of the microgrid [17]. A new approach for robust controller design described as coefficient diagram method has been implemented to reduce the deviations of frequency in an isolated power system powered by a photovoltaic panels and DGs [18].

The intermittency of solar radiation and wind speed causes remarkable frequency deviations in power systems connected with off shore wind energy generator and photovoltaic systems. Frequency deviations are minimized with the usage of different renewable energy sources along with BESS, flywheel energy storage systems and ultra capacitors [19].

Out of the literature reviews done so far it is observed that better tuning methods and control approaches are to be adopted to maintain the power balance and enhance frequency control in the microgrid. Hence this paper explores

the design and suitability of a PI controller tuned using internal model approach for enhanced dynamic performance and better frequency control.

The paper is organized as follows. Section II presents the microgrid configuration and modeling of the different sources in the microgrid for load frequency control. Section III and IV presents the design of PI and FOPI controllers using IMC method. Section V presents the dynamic simulation results for load frequency control performance. Section VI presents the sensitivity analysis of the microgrid frequency to parameter variations. Section VII presents the conclusion.

2. Microgrid Configuration and Modelling

The configuration of the hybrid microgrid system comprising of the following energy sources (i) WTG (ii) DG (iii) AE (iv) FC (v) BESS is shown in Fig. 1. The total power supplied to the load P_s is given by

$$P_s = P_{WTG} + P_{DG} + P_{FC} - P_{AE} \pm P_{BESS} \quad (1)$$

where P_{WTG} , P_{DG} , P_{FC} , P_{AE} are the output power of the WTG, DG, FC and P_{AE} is power input to the AE respectively.

In practical systems, DGs, FCs, and AEs are higher order models and have considerable degree of nonlinearity. However, for designing the controller a simplified transfer function model represented with a first order lag is utilized for the different energy sources comprising of DG, FC, AE and BESS as done in [1,2] is adopted in this paper.

2.1. Wind Turbine Generators

The mechanical power output of wind turbine is given by

$$P_w = 0.5\rho A_r C_p V_w^3 \quad (2)$$

where ρ is the density of air and its value is 1.25kg/m^3 . The swept area (A_r) of blades= 1735 m^2 [2]. C_p is a function of both tip speed ratio λ and blade pitch angle β . V_w is the velocity of the wind in m/s. The transfer function of the WTG is given by

$$G_{WTG}(s) = \frac{K_{WTG}}{1 + T_{WTG}s} \quad (3)$$

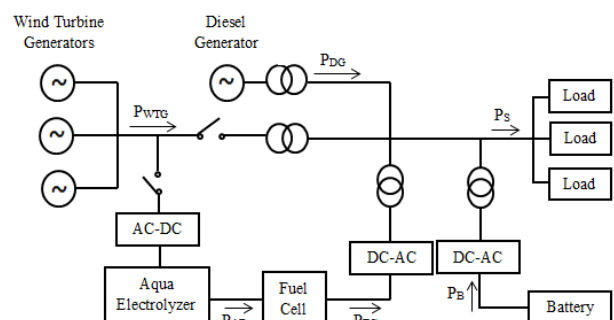


Fig. 1. System configuration

where K_{WTG} and T_{WTG} are the gain and time constants of the WTG respectively. The gain and time constants of the various sources are taken from [1] and presented in Table 4.

2.2. Diesel Generator Systems

The DG used in the microgrid model has features of quick start up and high efficiency. It consists of a diesel engine connected to a synchronous generator. Power deficits in the microgrid are balanced using the electrical output from the DG system. The DG output compensates for the increase or decrease of wind power in a shorter period. The transfer function of the DG is given by

$$G_{DG}(s) = \frac{K_{DG}}{1 + T_{DG} s} \quad (4)$$

where K_{DG} and T_{DG} are the gain constant and time constant of the DG respectively.

2.3. Fuel cell generator

The fuel cell is a power generating device which converts chemical energy into electrical energy. Electric power is generated in FC by the electrochemical reaction of the hydrogen gas produced by the aqua electrolyzer. The hydrogen fuel is divided into ions and electrons at the anode. The positively charged ions pass through the proton exchange membrane and the negatively charged electrons flow through the external circuit. The transfer function of the FC is given by

$$G_{FC}(s) = \frac{K_{FC}}{1 + T_{FC} s} \quad (5)$$

Where K_{FC} and T_{FC} are the gain and time constants of the FC respectively.

2.4. Aqua Electrolyzer Systems

The AE system is used because of the cleanliness of the hydrogen. As electrical power is sent to the two electrodes, hydrogen appears at cathode and oxygen appears at anode. A reduction reaction takes place in which the electrons combine with hydrogen ions to form hydrogen gas. The AE absorbs electrical energy from the renewable sources like wind or PV and produces hydrogen gas to feed the FC. The transfer function of AE is expressed as

$$G_{AE}(s) = \frac{K_{AE}}{1 + T_{AE} s} \quad (6)$$

where K_{AE} and T_{AE} are gain and time constants of the AE respectively.

2.5. Battery Energy Storage Systems

The BESS consists of a DC battery bank. The cells can be connected in series and parallel and the desired voltage level can be obtained. The BESS are capable of acting as a

load or as a generator. It discharges the power into the network as the frequency drops and charges when the frequency rises. It has relatively small time constant and has high reliability.

$$G_B(s) = \frac{K_B}{1 + T_B s} \quad (7)$$

where K_B and T_B are the gain and time constants of the BESS respectively. To find K_1, K_2, K_3 and K_4 refer [17].

2.6. Power and Frequency Deviations

The frequency should be maintained properly in the micro grid to ensure better quality of electricity delivery. To meet the required load demand P_s^* , the total power generation P_s must be effectively controlled by using appropriate controllers. The difference between the power demand and the generated power, ΔP_e is given by

$$\Delta P_e = P_s^* - P_s \quad (8)$$

As load demand varies, the system frequency Δf deviates. Δf is represented as

$$\Delta f = \Delta P_e / K_{sys} \quad (9)$$

where K_{sys} is the system frequency characteristic constant. The microgrid transfer function is expressed as [2]

$$G_{sys}(s) = \Delta f / \Delta P_e = 1 / K_{sys} (1 + s T_{sys}) = 1 / Ms + D \quad (10)$$

where M and D are inertia and damping constant respectively. The block diagram of the islanded hybrid microgrid system with transfer function [1,2] is shown in Fig. 2.

3. Design Procedure of IMC

For the load frequency controller design of microgrid, internal model control method (IMC) has been used. The structure of the IMC is given in Fig. 3a. $g(s)$ is the plant transfer function (in this case transfer function of different generating sources which are to be controlled), $\tilde{g}(s)$ is the plant model, $q(s)$ is the IMC controller; $r(s)$, $y(s)$ and $d(s)$ is the reference input, output and disturbance input to the plant respectively [20].

From Fig. 3a, it can be written as,

$$\tilde{y}(s) = \tilde{g}(s).u(s) \quad (11)$$

$$u(s) = q(s).e(s) \quad (12)$$

By replacing the value of $e(s)$ with $r(s)$, $y(s)$ and $\tilde{y}(s)$ in Eq. (12), we get

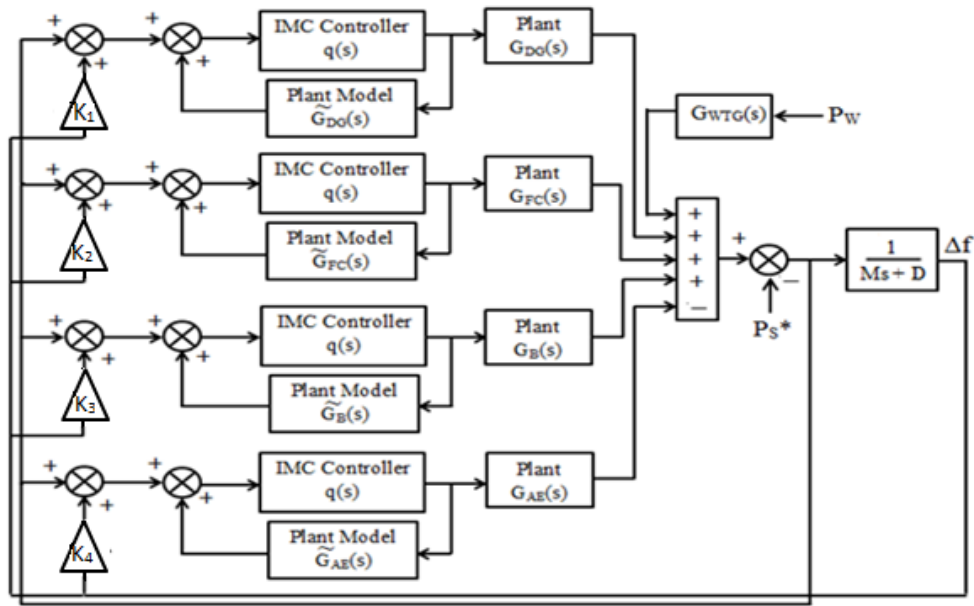


Fig. 2. Microgrid transfer function Model

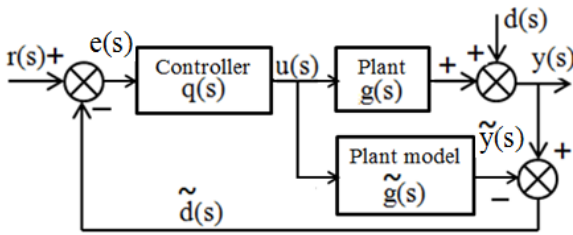


Fig. 3a. Structure of IMC

$$u(s)[1 - \tilde{g}(s).q(s)] = q(s) [r(s) - y(s)] \tag{13}$$

A system should exhibit good set point tracking; i.e. $r = y$, when $d=0$. Then the Eq. (13) becomes

$$1 - \tilde{g}(s).q(s) = 0 \tag{14}$$

$$q(s) = 1 / \tilde{g}(s) \tag{15}$$

Eq. (15) shows that the Internal Model controller transfer function is equal to the inverse of the plant model. If the microgrid plant model contains positive zeros, it results in an unstable system. If this problem exists, the following procedure is carried out to resolve it.

1) The plant model has been decomposed into two parts [21];

$$\tilde{g}(s) = g_m(s)g_a(s) \tag{16}$$

where $g_m(s)$ is the transfer function which contains the negative zeros and negative poles; $g_a(s)$ is the transfer function containing the zeros which have the mirror image of

the poles. The magnitude of $g_a(s)$ is made unity to ensure that there is no change in the plant model transfer function.

2) The IMC controller is designed such that the inverse of $g_m(s)$ is multiplied by the filter transfer function $f(s)$ and is given in Eq. (17). If the plant model contains dominant poles, it affects the steady state response of the system. Hence, the filter containing lead part is designed to offset the dominant poles.

$$q(s) = g_m^{-1}(s) f(s) \tag{17}$$

$$f(s) = \frac{1}{(\lambda s + 1)^x} \tag{18}$$

λ is the tuning parameter and x describes the order of the transfer function of $g_m(s)$ which consists of only negative zeros and negative poles. It is represented in Fig. 3b that the structure of IMC controller is comparable to that of any feedback control system having the IMC transfer function $q(s)$ in the forward path and plant model $\tilde{g}(s)$ in the feedback path of IMC. The overall transfer function comprising of IMC and the plant model $g_c(s)$ is given by

$$g_c(s) = q(s) / (1 - \tilde{g}(s)q(s)) \tag{19}$$

The procedure proposed for finding PID controller parameters using the IMC structure is as follows [21]

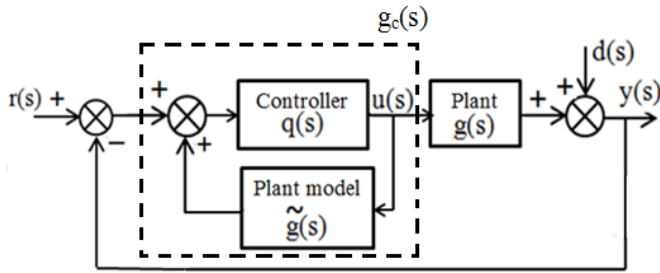


Fig. 3b. Feedback Structure

For any controller, compute the frequency response of $g_c(s)$

- 1) The frequency at which the magnitude of $g_c(s)$ has a minimum value is set as ω_h .
- 2) The PID values of the load frequency controller are obtained from

$$g_{pid}(s) = K_p + K_i/s + K_d(s) \quad (20)$$

such that

$$k_i = \text{imag} |g_c(j\omega)|^* \omega_h$$

$$k_p = \text{Re}(g_c(j\omega))$$

$$k_d = \text{imag}(g_c(j\omega)) / \omega_h$$

4. Design Procedure for FOPI using IMC

The fractional order PID (FOPID) controller is an improved version of conventional PID controller centered on fractional calculus.

The general representation of the FOPI controller is described as

$$g_c(s) = K_p + K_i / s^\gamma \quad (21)$$

where K_p is the proportional constant, K_i is the integral constant and γ is a fractional number.

The design procedure described in [22] is taken for finding the FOPI controller parameters. Consider a plant of first order system,

$$g(s) = n_o / (m_1 s + 1) \quad (22)$$

where n_o and m_1 are gain and time constants of the plant. Substituting Eq. (16) and Eq. (17) in Eq. (19), the controller for FOPI is obtained as

$$g_c(s) = g_m^{-1}(s) f(s) / (1 - f(s) g_a(s)) \quad (23)$$

By substituting the values of $g_m(s)$, $g_a(s)$ and $f(s)$ in Eq. (23) as stated for IMC procedure, the controller for FOPI is obtained as

$$g_c(s) = (m_1 s + 1) / n_o \lambda s \quad (24)$$

Rewriting the general representation of $g_c(s)$ as

$$g_c(s) = K(1 + 1/T_i s) \quad (25)$$

On comparing Eq. (24) with Eq. (25) the control parameters are obtained as

$$K = m_1 / n_o \lambda \quad \text{and} \quad T_i = m_1 \quad (26)$$

The value of γ is chosen arbitrarily. In this case, $g_m(s)$ is equal to $g(s)$.

5. Simulation Results

In this section, the contribution of WTG, DG, FC, AE and BESS are analyzed for load frequency control in the microgrid. The practical wind speed data taken from [23] is shown in Fig. 4a. Fig. 4b shows the variations of system electrical load. At 0s, the load is at 0.9 p.u. At 20s, the load is increased from 0.9 p.u. to 1.1 p.u. and decreased to 1 p.u. at 80s. The dynamic simulations are carried out for the disturbances specified. Using Eq. (2), the mechanical power of WTG is calculated which is displayed in Fig. 4c.

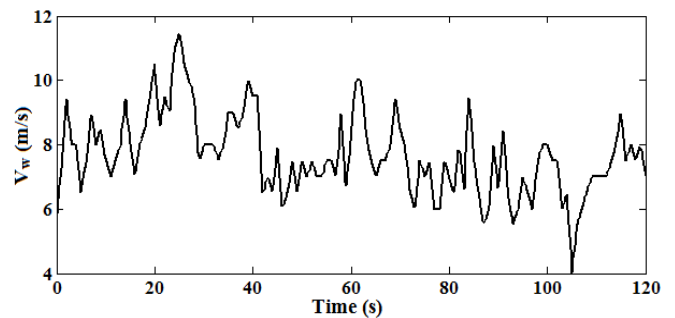


Fig. 4a. Wind Velocity

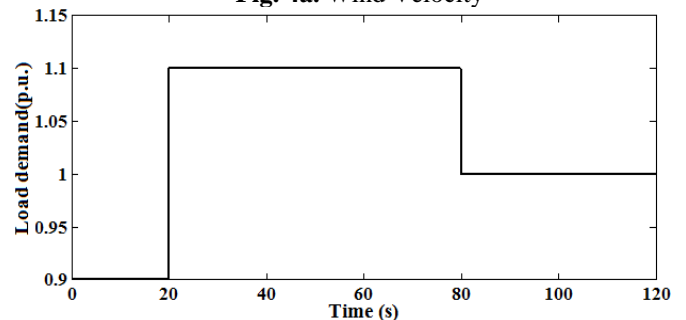


Fig. 4b. Variations of System load

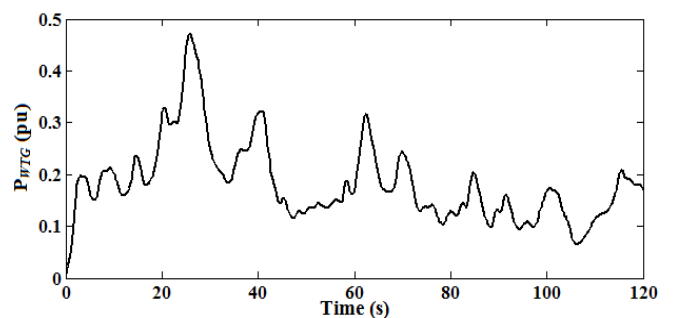


Fig. 4c. Wind Turbine Generator output

In Fig. 4d, the variations of DG output for different set of controller methods are presented. At 0s, the load is 0.9 p.u. The DG raises its output and takes part in load frequency control as evident from the zoomed portion noted in Fig. 4d. It is found that DG output shoots up to 0.77 p.u. and 0.75 p.u. for IMC tuned FOPI and PI controllers respectively.

At 20s, the system load is increased from 0.9 p.u. to 1.1 p.u. The DG increases its output to compensate for the load frequency control. The wind velocity also increases at 20s which results in increased WTG output. The increased WTG output can be utilized for better frequency regulation. Since all the energy sources are interconnected in the model, the DG increases its electrical output. At 80s, the load is reduced from 1.1 p.u. to 1 p.u. Subsequently, the DG reduces its output. The WTG output is such that it maintains the real power balance in the system.

At time $t = 0s$, the system electrical load is 0.9 p.u and the FC generates the required power in order to maintain the nominal frequency. The FC electrical output shoots upto 0.34 p.u. and 0.37 p.u. for the IMC tuned FOPI and PI controllers which is shown in Fig.4e. At 20s, the load is increased from 0.9 p.u. to 1.1 p.u. The WTG output is also increased. Since the WTG output is not sufficient to control the frequency deviations, the FC increases its output. At 80s, the FC reduces its power output since the load is dropped to 1 p.u.

The variation of the AE output power is shown in Fig. 4f. The AE absorbs the essential electrical power and generates hydrogen to supply the FC. At 0s, it is found that AE output

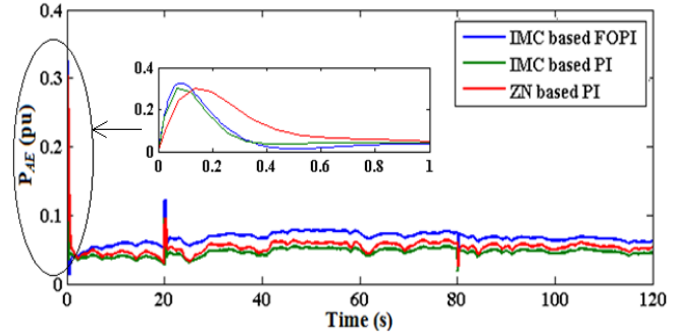


Fig. 4f. Aqua Electrolyzer output

increases to 0.32 p.u. and 0.3 p.u. for IMC tuned FOPI and PI controllers. At 20s, the load is increased to 1.1 p.u. the AE has generated the required electrical power. At 80s, the load has been dropped to 1 p.u., the AE generates less power.

The variation of the BESS power output is shown in Fig. 4g. At 0s, the microgrid system experiences a load of 0.9 p.u. As the generating power from all the energy sources are inadequate, the BESS discharges the electrical power to maintain the nominal frequency. At 20s, it increases its electrical output so as to meet the load demand of 1.1 p.u. At 80s, the load has been dropped to 1 p.u. which results in surplus power generation and the BESS enters into the charging mode.

Fig.4h shows the frequency deviation of the microgrid system for different loading conditions. As the demand is not satisfied by the generating sources, the system experiences a slight variation in the nominal frequency. Because of a load increase and decrease at 20s and 80s, frequency deviations increase and decrease. With the intervention of energy sources, the frequency deviation is reduced nearly to zero within a short time period.

The peak overshoot of the frequency deviation with the proposed IMC based FOPI and PI controllers are -0.128Hz and -0.143Hz which are lesser than the PI controller tuned by Ziegler-Nichols(ZN) method having peak overshoot of -0.195Hz at 0.1s. With the proposed method, the system settling time is very less with 0.3s compared with the ZN method with 1.5s. This shows the improvements brought out by the IMC based FOPI and PI controllers in the system dynamic response.

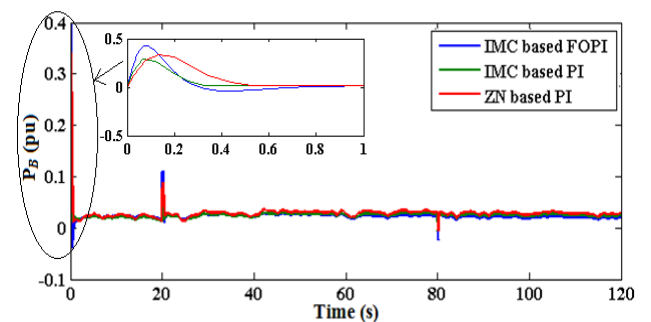


Fig. 4g. Battery charging and discharging Power

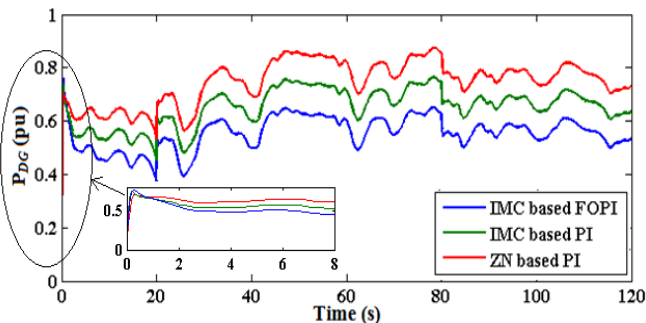


Fig. 4d. Diesel Generator Output

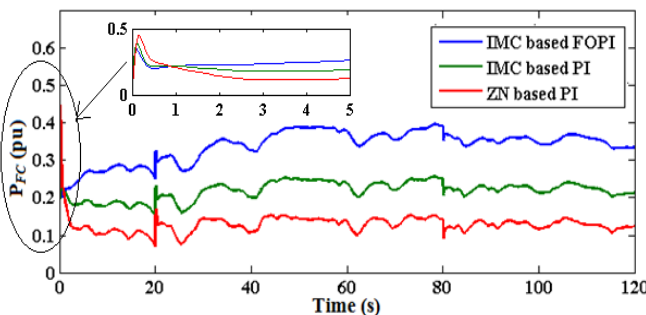


Fig. 4e. Fuel Cell output

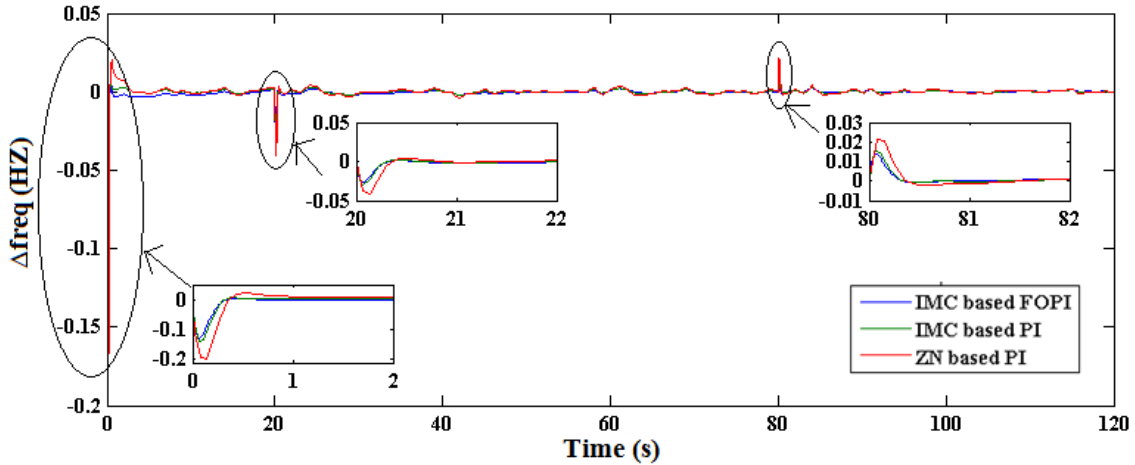


Fig. 4h Frequency deviation of the Microgrid System

6. Sensitivity Investigation

Sensitivity investigations are carried out to analyze the capability of the micro grid system subjected to parameter variations. The time constants of the DG, FC, AE and BESS are varied $\pm 25\%$ from their nominal values in order to evaluate the robustness of the controllers without changing the optimum values of controller gains.

Fig. 5 demonstrates the frequency variations of the microgrid with IMC tuned PI controllers for parameter variations. The performance indices like ISE (Integral Square Error), peak overshoot and settling time for the frequency deviation are given in Table I with IMC tuned PI Controller. It is observed that the response of the system has not shown considerable difference for the parameter variations.

The frequency deviation for the $\pm 25\%$ parameter

variation of the sources with FOPI controllers is shown in Fig. 6. The performance index ISE for the nominal parameter at 1s is 0.0021. With +25% parameter variation, the ISE is 0.0031. With -25% parameter variation, the ISE is 0.0013. Hence, for the $\pm 25\%$ parameter variation, the ISE values have not shown much difference. The peak overshoot, settling time and ISE values for the microgrid frequency deviation are given in Table II with IMC tuned FOPI controllers. Hence, the optimal values of the controllers need not to be retuned for the parameter variation.

The peak overshoot differs appreciably for the Ziegler Nichols tuned PI controller with that of the PI Controller tuned using IMC method [refer Tables 1,2 and 3]. Hence, it can be established that the proposed IMC control method of PI tuning is responsible for the robustness of the controllers when the system experiences parameter variations.

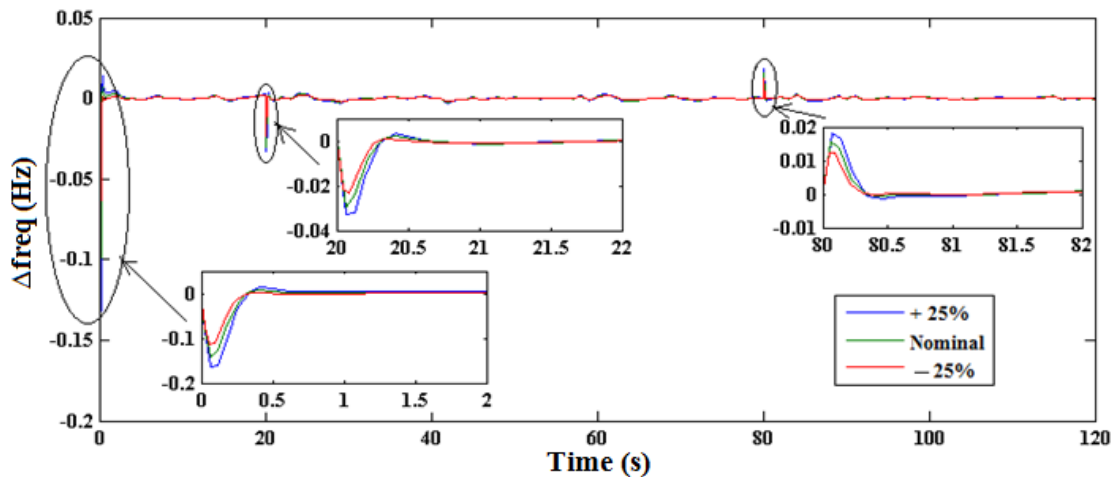


Fig.5 Frequency deviation for $\pm 25\%$ parameter variation of various sources for the IMC tuned PI controllers.

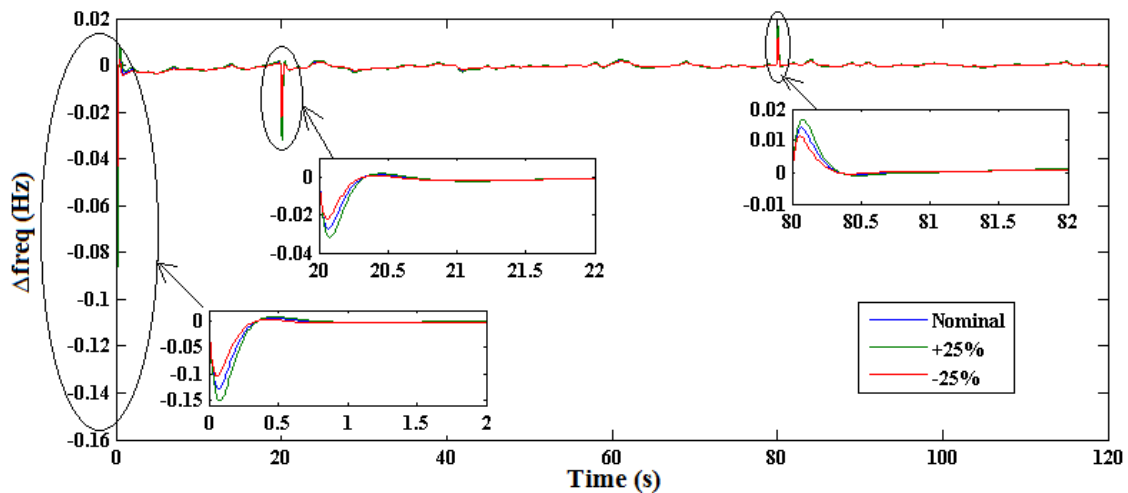


Fig. 6 Frequency deviation for $\pm 25\%$ parameter variation of various sources for the IMC tuned FOPI controllers

Table 1. Sensitivity analysis for $\pm 25\%$ parameter variation of various sources with IMC tuned PI controllers

| Performance index | Parameter Variations(T_{DG} , T_{FC} , T_{AE} , T_{BESS}) | | |
|-------------------|---|--------|--------|
| | Nominal | -25% | +25% |
| ISE | 0.0032 | 0.0016 | 0.0041 |
| Peak Overshoot | -0.155 | -0.113 | -0.165 |
| Settling Time(s) | 1.510 | 1.310 | 1.720 |

Table 2. Sensitivity analysis for $\pm 25\%$ parameter variation of various sources with IMC tuned FOPI controllers

| Performance index | Parameter Variations(T_{DG} , T_{FC} , T_{AE} , T_{BESS}) | | |
|-------------------|---|--------|--------|
| | Nominal | -25% | +25% |
| ISE | 0.0021 | 0.0013 | 0.0031 |
| Peak Overshoot | -0.128 | -0.104 | -0.151 |
| Settling Time(s) | 0.910 | 0.820 | 1.000 |

Table 3. Sensitivity analysis for the $\pm 25\%$ parameter variation of various sources with ZN tuned PI controllers

| Performance index | Parameter Variations(T_{DG} , T_{FC} , T_{AE} , T_{BESS}) | | |
|-------------------|---|---------|---------|
| | Nominal | -25% | +25% |
| ISE | 0.0071 | 0.0041 | 0.0106 |
| Peak Overshoot | -0.2000 | -0.1600 | -0.2400 |
| Settling Time(s) | 3.0 | 2.9 | 3.2 |

Table 4. Gain and Time Constants of the Micro Grid sources[1]

| | |
|------------------------------------|--------------------------------------|
| $K_{WTG} = 1$ and $T_{WTG} = 1.5s$ | $K_{FC} = 1$ and $T_{FC} = 4s$ |
| $K_{DG} = 1$ and $T_{DG} = 2s$ | $K_{BESS} = 1$ and $T_{BESS} = 0.1s$ |
| $K_{AE} = 1$ and $T_{AE} = 0.2s$ | $M = 0.2$ & $D = 0.012$ |

7. Conclusion

An IMC based load frequency controller has been designed for a microgrid system comprising of the WTG, DG, FC, AE and BESS. During the load variations, all the energy sources coordinated well in order to maintain the frequency to the nominal value. The BESS also improves the frequency control by delivering active power instantly. The simulation result shows that FOPI and PI controllers tuned using IMC method have outperformed well compared to Ziegler Nichols method. To the best knowledge of the authors, such an Internal Model Control application described in this paper to microgrid frequency control has not been attempted. The robustness of the controllers has been examined through the parameter variations of the DG, FC, AE and BESS. This inherent advantage of using IMC is due to the fact that the controller transfer function is made the inverse of the plant transfer function which results in better set point tracking and robustness. It is observed that the tuned values of controllers using IMC are robust for different loading conditions and parameter variations.

References

- [1] T. Senjyu, T. Nakaji, K. Uezato, and T. Funabashi, "A hybrid power system using alternative energy facilities in isolated island," IEEE Trans. Energy Conversion, vol. 20, no. 2, pp. 406–414, June 2005. (Article)
- [2] Dong-Jing Lee and Li Wang, "Small-Signal Stability Analysis of an Autonomous Hybrid Renewable Energy Power Generation/Energy Storage System Part I: Time-

- Domain Simulations”, IEEE Trans. Energy Conversion, vol.23, no.1, pp.311-320, March 2008.(Article)
- [3] K.V. Vidyanandan, Nilanjan Senroy, “Frequency regulation in a wind–diesel powered microgrid using flywheels and Fuel Cell”, IET Generation Transmission Distribution, Vol. 10, no. 3, pp. 780–788,2016. (Article)
- [4] I.Serban, C.Marinescu, “Battery energy storage system for frequency support in microgrids and with enhanced control features for uninterruptible supply of local loads”, Electrical Power and Energy System, vol.54, pp.432-441, Jan 2015. (Article)
- [5] E.Alexandre Oudalov, Daniel Chartouni, and Christian Ohler, “ Optimizing a Battery Energy Storage System for Primary Frequency Control”, IEEE Trans. Power System, Vol. 22, no. (Article)
- [6] Abdul Motin Howlader, Yuya Izumi, Akie Uehara, Naomitsu Urasaki, Tomonobu Senjyu, Atsushi Yona, Ahmed Yousuf Saber, “A minimal order observer based frequency control strategy for an integrated wind-battery-diesel power system”, Energy, vol .46, no.1, pp. 168-178, October 2012. (Article)
- [7] I.Serban, C.Marinescu, “Aggregate load-frequency control of a wind-hydro autonomous microgrid”, Renewable Energy, vol. 36, no.12, pp. 3345-3354, December 2011. (Article)
- [8] Yi Han, Peter Michael Young, Abhishek Jain, Daniel Zimmerle, “Robust Control for Microgrid Frequency Deviation Reduction With Attached Storage System”, IEEE Trans. Smart Grid, vol. 6, no.2, pp. 557–565, March 2015. (Article)
- [9] M.Khalid, A.V. Savkin, “An optimal operation of wind energy storage system for frequency control based on model predictive control”, Renewable Energy, vol.48, pp.127–32, December 2012. (Article)
- [10] Geeta Pathak, Singh, Bijaya Ketan Panigrahi. Control of Wind-Diesel Microgrid Using Affine Projection-Like Algorithm”, IEEE Trans. Industrial Informatics, vol. 12, no. 2, pp. 524-531, April 2016. (Article)
- [11] Mousa Marzband, Maziar Mirhosseini Moghaddam, Mudathir Funsho Akorede, Ghazal Khomeyrani, “Adaptive load shedding scheme for frequency stability enhancement in microgrids”, Electric Power Systems Research, vol.140, pp.78–86, November 2016. (Article)
- [12] Hassan Bevrani, Mohammad Ramin Feizi and Sirwan Ataee, “Robust Frequency Control in Islanded Microgrid: H_∞ and μ -Synthesis Approaches”, IEEE Trans Smart Grid, vol. 7, no. 2, pp.706-717, March 2016. (Article)
- [13] Mohammad Reza Khalghani, Mohammad Hassan Khooban, Esmaeil Mahboubi-Moghaddam, Navid Vafamand, Mohammad Goodarzi, “A self-tuning load frequency control strategy for microgrids: Human brain emotional learning,” Electrical Power and Energy Systems, vol.75, pp.311-319, February 2016. (Article)
- [14] H. Bevrani, F. Habibi, P. Babahajyani, M. Watanabe and Y. Mitani, Intelligent Frequency Control in an AC Microgrid: Online PSO-Based Fuzzy Tuning approach”, IEEE Trans. Smart Grid, Vol. 3, No. 4, pp.1935-1943, Dec 2012. (Article)
- [15] Cuk Supriyadi, Ali Nandar, “Robust PI control of smart controllable load for frequency stabilization of microgrid power system”, Renewable Energy, vol. 56, pp. 16-23, August 2013. (Article)
- [16] Xiangjun Li , Yu-Jin Song, Soo-Bin Han, “ Frequency control in micro-grid power system combined with electrolyzer system and fuzzy PI controller”, Journal of Power Sources, vol. 180, no.1, pp. 468–475, May 2008. (Article)
- [17] G. Mallesham, S. Mishra, and A. N. Jha, “Ziegler-Nichols based Controller Parameters Tuning for Load Frequency Control in a Microgrid”, Int. conf Energy, Automation and signal(ICEAS), pp.1-8, 2011. (Conference Paper)
- [18] Raheel Ali, Tarek Hassan Mohamed , Yaser Soliman Qudaih, Y. Mitani ,“ A new load frequency control approach in an isolated small power systems using coefficient diagram method”, Electrical Power and Energy Systems, vol. 56, pp. 110–116, March 2014. (Article)
- [19] Prakash K. Ray, Soumya R. Mohanty, Nand Kishor, “Proportional–integral controller based small-signal analysis of hybrid distributed generation”, Energy Conversion and Management, vol. 52, no.4, pp. 1943–1954, April 2011. (Article)
- [20] M. Morari and E. Zafiriou, Robust Process Control. Englewood Cliffs, NJ: Prentice-Hall, 1989. (Book)
- [21] W. Tan, “Unified Tuning of PID Load Frequency Controller for Power Systems via IMC”, IEEE Trans. Power Systems, vol.25, no.1, pp.341-350, Feb 2010. (Article)
- [22] Mahsan Tavakoli-Kakhki, Mohammad Haeri, “Fractional order model reduction approach based on retention of the dominant dynamics: Application in IMC based tuning of FOPI and FOPID controllers”, ISA Transactions, vol. 50, pp.432–442, March 2011. (Article)
- [23] http://renknownet2.iwes.fraunhofer.de/pages_en/objektdatenbank_en.htm (Website)